Analyst

Accepted Manuscript

ROYAL SOCIETY OF CHEMISTRY

www.rsc.org/analyst

Comparison of transflection and transmission FTIR imaging measurements performed on differentially fixed tissue sections

David Perez-Guaita[a,b], Philip Heraud[a,e], Katarzyna M. Marzec [a,c], Miguel de la Guardia[b], Matti Kiupel[d], Bayden R. Wood[a] *

[a]Centre for Biospectroscopy, School of Chemistry, Monash University, Clayton, 3800 Victoria., Australia.
[b]Analytical Chemistry Department, University of Valencia, Edifici Jeroni Muñoz, 46100 Burjassot, Spain
[c]Jagiellonian Centre for Experimental Therapeutics, Jagiellonian University, 30348 Krakow, Poland
[d] Diagnostic Center for Population and Animal Health, 48910-8107 Lansing (MI), USA
[e]Department of Anatomy and Developmental Biology, Faculty of Medicine, Monash University, Clayton, 3800 Victoria., Australia.

Corresponding author: bayden.wood@monash.edu

Abstract

The widespread and cost-effective use of transflection substrates in Fourier transform infrared (FTIR) imaging of clinical samples is affected by the presence of artefacts including the electric field standing wave (EFSW) and contributions from light dispersion. For IR-based diagnostics, the manifestation of undesirable artifacts can distort the spectra and lead to erroneous diagnosis. Nevertheless, there is no clear consensus in the literature about the degree of influence of these effects. The aim of this work is to contribute to this discussion by comparing transflection and transmission images of the same tissue. For this purpose two adjacent sections of the same tissue (lymphoma sample) were fixed onto a CaF_2 window and a transflective slide for FTIR imaging. The samples in this case had a central area where based on morphology it was presumed the fixative did not penetrate to the same extent hence providing a comparable region for the two different substrates with a distinct physical/chemical difference. Transmission and transflection spectra from adjacent hyperspectral tissue images were combined in an extended dataset. Surprisingly, unsupervised hierarchical cluster analysis clustered together transflection and transmission spectra, being classified according to differences in tissue fixation instead of the geometry employed for the image acquisition. A more detailed examination of spectra from the peripheral zone of the tissue indicated that the main differences between the transflection and transmission spectra were: 1) a small shift of the amide I, 2) a larger "noise" component in the transflection spectra requiring more averaging to obtain representative spectra of tissue types, and 3) the phosphate bands were generally higher in absorbance in the transflection measurements compared to the transmission ones. The amide I shift and the larger spectral variance was consistent with results obtained in

previous studies where the EFWS was present. The findings indicate that artifacts resulting from transflection measurements were small but consistent across the tissue, and therefore the use of transflection measurements could be employed for disease diagnosis. Accordingly, we recommend a straightforward multivariate comparison of images from transmission and transflection measurements in a combined data matrix obtained from adjacent sections of the tissue as a useful preliminary study for establishing the impact of the EFWS on the samples, before considering the routine use of transflection substrates for any new tissue studied.

Introduction

Fourier transform infrared (FTIR) spectroscopy shows potential as a diagnostic tool for clinical samples, providing useful information about the presence, concentration and structure of different macromolecules within those samples. The technique has become a promising tool for the diagnosis of different diseases, including cancer, [1] renal failure[2] and endometriosis[3] because of the large amount information that can be extracted from FTIR spectra and the potential for automated diagnosis. In addition, the introduction of advanced focal plane array detectors and powerful sources have permitted the rapid and easy acquisition of hyperspectral microscopic images with high-quality IR spatial information. Previous studies have shown that by combining infrared microspectroscopy with chemometric techniques, multivariate models can be generated for the characterization of tissue samples including cervical cancer, prostate cancer, brain cancer, heart tissue and liver disease.[4]

Infrared imaging measurements on tissues are often performed in transflection instead of transmission mode because of the cost-effectiveness of the reflective substrates compared to IR transparent windows including CaF_2, BaF_2, ZnSe and KRS-5. This becomes a serious issue especially when dealing with large patient sample numbers and replicate sections. However, the use of transflection substrates particularly for single cell analysis has been recently questioned by Filik et al.[5] because of spectral variation induced by the Electric field standing wave (EFSW) artifact on the transflection measurement.[6] This effect, a well-known property of the light[7] observed for example in the study of adsorbed molecules onto metal surfaces[8], introduces non-linear absorptions in infrared spectra. In the study of Filik et al. this effect was quantitatively studied and modelled through different wavenumber values and thicknesses on single cells and proteins films demonstrating dramatic differences between transmission and transfection spectra. This effect has been also recently studied and theoretically modeled by Bassan et al.[9], where the authors, using a

prostate tissue sample, alerted to the problems that the EFSW can potentially introduce in the classifications of tissue. They also stated "..that preparing tissue at a consistent thickness using a microtome negates the transflection thickness problem are not valid", due to the dependence of the EFSW with both, the particle size and refractive index and to small variations of the tissue induced by instrumental error of the microtome. In contrast, Wrobel et al. claimed that this effect is diluted with some experimental factors inherent to the transflection system, such as the "integration over the range of incidence angles, varying degrees of coherence of the source and heterogeneity in sample thickness" and concluded that "the results indicate that the significant body of work over the past two decades on such substrates is not necessarily invalid".[10] It seems therefore that the impact of the EFSW depends on the particular analytical problem under study, and therefore it is important to establish if it can interfere with the reliability of the results obtained. The importance of this discussion is critical for diagnosis based on transflection measurements, where the biological variations connected with the illness could be hindered by the spectral variations related to the thickness of the sample introduced by the EFSW and other spectral artefacts such as scattering or reflection contributions.

Transflection and transmission measurements require different substrates and therefore it is impossible to prepare the same sample in exactly the same manner for both measurement geometries. For this reason we followed the same approach developed for performing three-dimensional multivariate image analysis of adjacent tissue sections[11]: Two adjacent sections of the same tissue (lymphoma sample) were fixed onto a CaF_2 window and a MirrIR slide and then imaged using transmission and transflection geometries, respectively. The choice of tissue in this case was a canine lymphoma sample, which is very homogenous in terms of cell type and chemistry excepting for a central area where the fixative did not quite penetrate creating a chemical environment different to the periphery of the tissue. A third adjacent section was fixed on a regular glass slide and H&E stained for a photomicrograph reference. Images and spectra were compared using unsupervised hierarchical cluster analysis (UHCA) and principal components analysis (PCA) in order to identify similarities and differences between transmission and transflection measurement modes and to assess the effect of the EFSW and other 'artifacts' on the transflection spectral images. We compared UHCA maps from fixed and sectioned canine lymphoma tissue using transmission and transflection substrates by combining the data sets in the same data matrix prior to UHCA and demonstrate that the ESFW is not a significant contributor to achieving consistent registration of inter- and intra-section chemical differences in tissue sections.

Experimental

Lymphoma samples

Serial sections from two lymphoma samples were cut with a microtome following routine methods. Adjacent sections from each lymphoma case were fixed onto a regular glass slide, a CaF_2 window and a high reflective MirrIR slide from Kevely Technologies (Chesterland, OH, USA) each for the acquisition of visible, transmission infrared and transflection infrared image acquisition. The tissue placed on the glass slide was sectioned to 4 µm, fixed and stained with Haematoxylin-Eosin (H&E). In order to keep approximately the same path length, tissues destined for transflection and transmission IR measurements were sectioned at 4 and 8 µm thickness, respectively, and then transferred onto the substrates. Samples were deparaffinized prior to the IR measurement by three consecutive 5-minute washes in xylene.

FTIR imaging

Hyperspectral infrared images were acquired using a Cary 620 FTIR microscope system from Agilent Technologies (Mulgrave, Victoria, Australia) equipped with a 128 × 128 pixel FPA (mercury-cadmium-telluride) detector using a 32 x Cassegrain objective. Spectra were recorded over the spectral range 3800-950 cm^{-1} at a spectral resolution of 4 cm^{-1} by co-adding 4 interferograms. Single images (8x8) were recorded by binning 16 pixels. Tissue sections were imaged as a 625-tile mosaic (25 × 25). The final mosaic images had dimensions of 200 × 200 pixels covering an area of approximately 4 cm^2 (2 cm × 2 cm). Resolutions Pro software from Agilent was used for the acquisition, handling of the spectra and composition of the mosaic images. Visible images were acquired using a WITec confocal CRM alpha 300 Raman microscope (WITec Instruments Corp., Knoxville, TN, USA), using the digital camera and taking advantage of the high precision piezo electric stage.

Data treatment

FTIR mosaic images were imported into Cytospec software,[12] where the spectral range was cut to only include the fingerprint region (1800-950 cm^{-1}) and a quality control applied to remove background pixels where there was no tissue absorbance. A first UHCA was performed on the individual images using Cytospec routines. Then the images were exported as a 3-D matrix to Matlab 7.7.0 (Mathworks Inc., Natick, MA, USA), where the transflection and transmission images

of the same sample were included together on an augmented data matrix with dimensions of 400 x 200 pixels (transmission and transflection image dimensions upwards and downwards, respectively). The augmented data matrix was again loaded into Cytospec and UHCA was performed over the augmented image composed of the transflection and transmission images, using a Savitsky-Golay derivative (order: 2, number of smoothing points: 11) for spectral preprocessing. UHCA was based on Euclidean distance and performed using the shortcut available on Cytospec™.

PLS Toolbox 7.0 from Eigenvector Research Inc. (Wenatchee, WA, USA) and in-house written Matlab functions were used for the PCA. The preprocessing steps used for each PCA are detailed in the results section.

Results

Comparison between transflection and transmission images

UHCAs performed on individual images can be seen in Supplementary Figure 1 and Supplementary Figure 2. It can be observed that a similar classification was achieved for both modes, excluding the green class of tissue #2, which in transmission image covered a larger part of the tissue. In order to study the general similarities and differences between the IR images obtained by transflection and transmission measurements, we performed other UHCA from the spectra of an extended data matrix including together spectra from both the images obtained by transflection and transmission. Cluster analysis is a widely used method in hyperspectral imaging which groups the spectra according to their general similarities. Figure 1 shows a comparison between the image of the stained tissues and the images obtained from the cluster classification performed on the FTIR spectra, obtained from transmission and transflection measurements. FTIR microscopic images are superimposed over the stained images, and the colour of each pixel is coloured according to the class defined by the cluster. The three images are not exactly the same because of differences in the efficiency of the fixation, and changes in the three dimensional tissue architecture, but it is clear that there is generally good correspondence between images obtained from adjacent sections from the microtome.

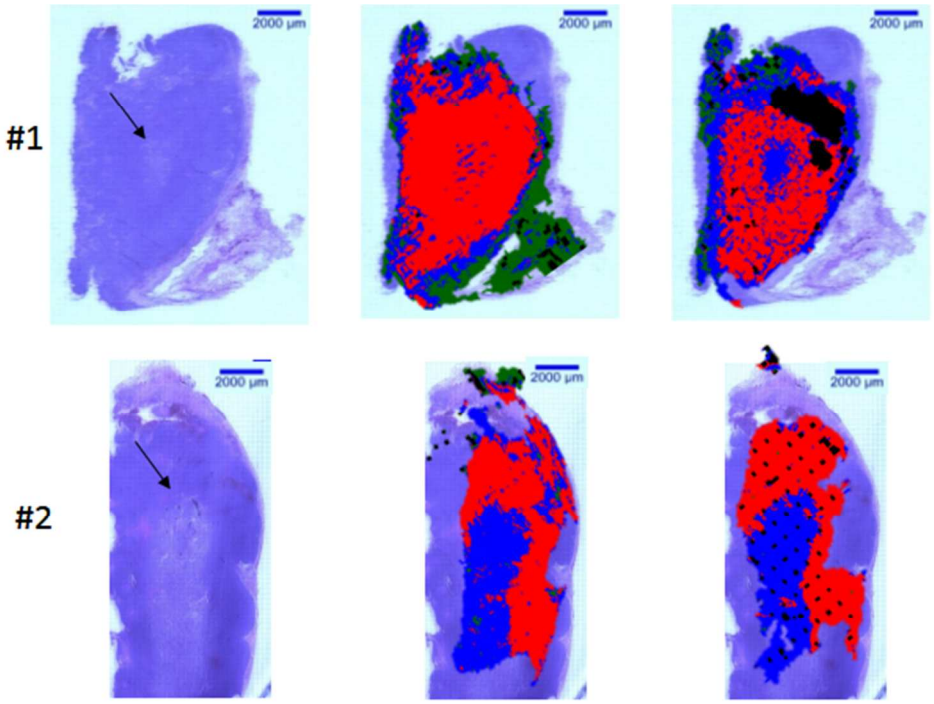

Figure 1. Comparison between transflection and transmission measurements of two lymphoma samples: Visible image of H&E stained tissue (left) and infrared images measured by transmission (center) and transflection (right), with the pixels colored according to the class determined by the unsupervised hierarchical cluster analysis performed on combined data matrix including spectra from both transmission and transflection images. Black pixels represent spectra that have not passed the quality test performed in Cytospec, based on the integrated area under bands in the 1400-1700 cm^{-1} region.

One expects that, if there is a critical impact of the artifacts associated with the transflection measurement the clusters obtained would have clearly separated for transflection and transmission modes. It can be seen that the classification obtained by the cluster analysis shows a radial distribution of the classes, related with zones of the tissue that were fixed differently instead of the measurement mode. This distribution is more evident on #1 than #2 due to problems of fixation efficiency. For a better understanding of the composition of this radial distribution the mean spectra of each class are shown in Figure 2. In both cases there is a group composed of spectra with low absorbance, coloured in green, which corresponds to a small area of material at the edges of the tissues. The red class corresponds to an area inside the green coloured region and peripheral to the central region of the tissue, and it is connected with the highest absorbance spectra. The blue class corresponds to the internal edge and the center of the tissue, and we assigned this area to zones with

a medium efficiency of fixation, as shown in the spectra with a mean absorbance in the middle of the other groups of spectra. This grouping is consistent with the information provided by the histology team, which reported low fixation efficiency in the middle of the tissue as compared with the peripheral tissue zone. This phenomenon is also observed on the images of the stained tissue, which shows a more transparent zone in the central region of the tissue. A more detailed inspection of this zone with higher magnification showed the existence of holes within this region. A full resolution micrograph of one of the tissues showing these physical features is shown in Supplementary Figure 3.

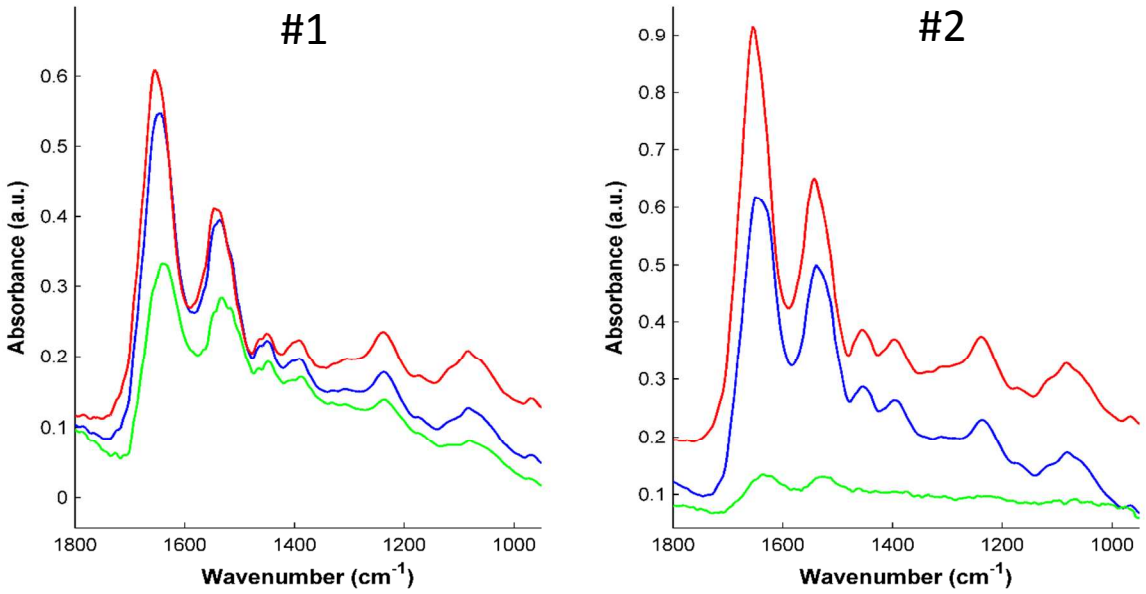

Figure 2. Mean spectra of the classes defined by the cluster analysis performed on the IR images of the sample #1 and #2.

Most importantly, it is clear that there are strong similarities between the images obtained from the transmission and transflection measurements. Naturally one expects there to be differences in the images and spectra for a number of reasons: 1) the sample thickness is doubled for transmission compared to transflection measurement and those differences on the thickness imply changes in Mie scattering, 2) tissue #1 is slightly wider for the transflection measurement, 3) the tissues employed for the transflection and transmission measurements are adjacent and not identical, 4) there are differences induced by the process of cutting and fixation. However, for both samples, the cluster analysis classified into separate classes the center, edges and peripheral zones from the IR images obtained in both transmission and transflection modes. In summary, the classification

obtained on the clustering procedure, which classifies the same groups of transflection and transmission spectra from the same regions of the tissue into the same classes clearly shows that the differences between the tissue regions due to fixation are larger than the differences between the transflection and transmission measurements.

Whether or not EFSW, Mie scattering or other artefacts are present in the transflection measurements of the lymphoma samples cannot be established from the cluster analysis alone. The main conclusion from UHCA is that any of these effects are not critical when considering the distribution of the chemical differences induced by the differing extent of tissue fixation. For identifying the presence of any of these artifacts, a deeper study is required comparing the spectra obtained from the same region using transflection and transmission measurements, which is delineated below.

Differences between the transmission and transflection spectra of the peripheral area

Since the peripheral area of the tissues showed the highest absorbance and homogeneity, this region was selected for performing the spectral comparison between transflection and transmission modes. For each lymphoma sample, 20 spectra were randomly selected from the red region representing this peripheral tissue zone from both the transflection and transmission mode data, resulting in two data sets of 40 spectra. In order to ensure that there were no outliers among those samples a PCA was performed in order to see if any of the selected samples showed unusual Q^2 and T^2 values. An overview of the raw spectra (See figure 3a) showed that some of those transflection spectra were shifted on the absorbance-axis, which indicated the presence of some transflection associated artifacts. The origin of this shift was not clear, but in the aforementioned cluster analysis it was presumably corrected by the derivative in the HCA. After several preprocessing steps, including smoothing, linear baseline subtraction (See supplementary Figure 4 for more information) and normalization, the transflection spectra appeared quite similar to the transmission ones (See figure 3b).

Nevertheless, a simple visual inspection still showed some differences between transflection and transmission spectra. For example transflection spectra show larger variance in bands at 1390 and 1460 cm^{-1}, which can be attributed to an EFWS artifact or to a larger relative error in tissue sectioning. The fact that some of the transflection spectra exhibited higher absorbance at ~1240 cm-1 and ~1085 cm^{-1} assigned to the symmetric and asymmetric phosphodiester vibrations is unclear.

One possible explanation is that the EFSW increases the absorbance of the lower wavenumber region of the spectra, but this explanation does not fit with the fact that bands at 1390 and 1460 cm^{-1} are not affected by this enhancement. Excluding the variance and the phosphate bands, the transflection spectra were easily superimposed with the transmission ones. From visual inspection, we ascertain that the effects of the EFWS are not critical and are similar in the entire peripheral area, probably caused by the high homogeneity of the samples both in terms of cell and organelle size and refractive index of the tissue. Moreover, it has to be noted that the experimentally observed absence of a clear EFWS effect on the fingerprint region could not be extrapolated to higher wavenumber regions in the spectra.

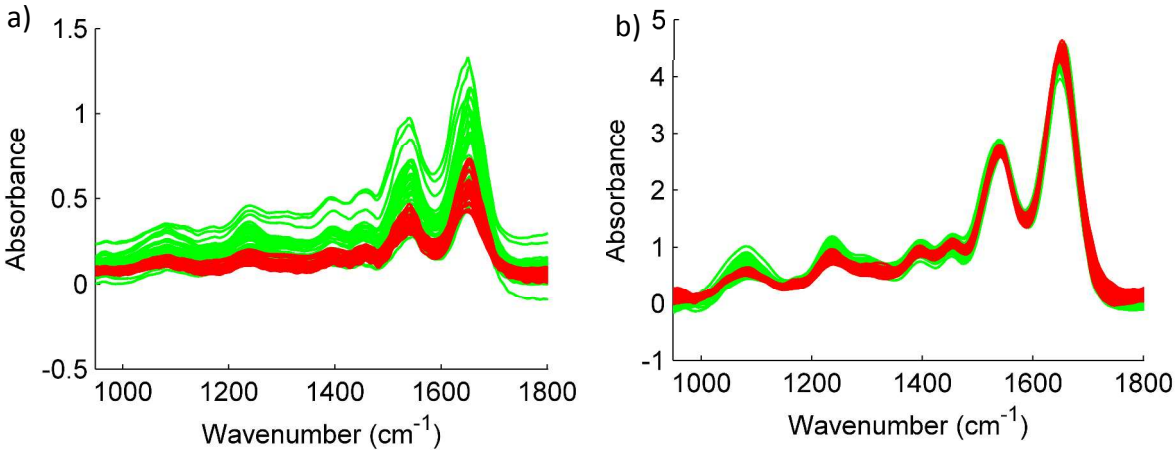

Figure 3. Transmission (red) and transflection (green) spectra randomly selected from the peripheral zone: a) raw spectra and b) spectra after smoothing (polynomial order: 0 and smoothing points: 7), baseline subtraction (See SM4) and normalization (Standard Normal Variate).

For a deeper look into the spectral differences between the transmission and transflection spectra, PCA was applied. Figures 4a and 4b shows the PC1 Score Plots of the spectra (after smoothing, baseline correction and mean centering) for the two lymphoma samples under study. In both cases, the first PC is able to capture the main variance of the system (73 and 90 % respectively), and in both cases this new variable is connected with the differences between transflection and transmission measurements. Spectra measured through transmission presented higher score values than those obtained for the spectra measured through transflection. However, the study of the PC1 Loadings Plot (Figure 4c) shows that those differences are related to changes on the general fingerprint of the tissue. We argue that this behavior can be caused by a different pathlength resulting from variations in tissue thickness introduced by instrumental error of the microtome.

Tissue samples were sectioned with the aim to ensure a similar pathlength for transmission and transflection measurements. In transflection measurements the pathlength is doubled, so the sections were microtomed to half the thickness of the transmission measurement sections. Orientation effects and variations in thickness resulting from the cutting process could explain the separation observed on the PCA.

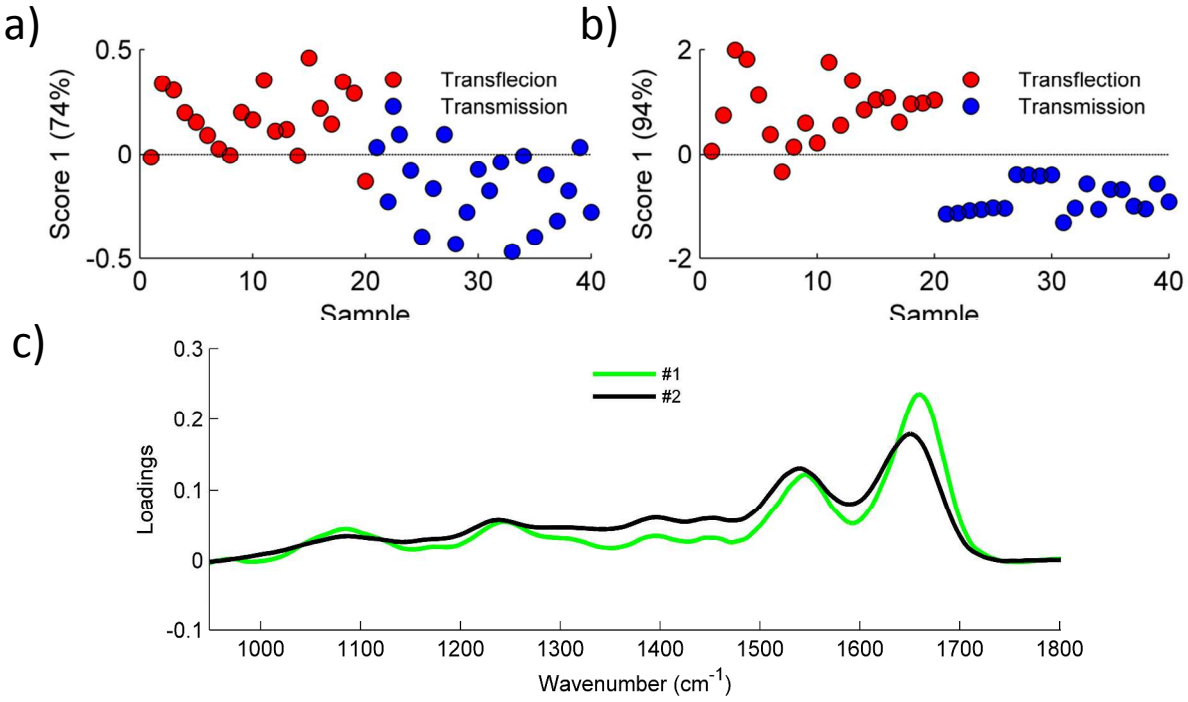

Figure 4. PCA performed over the transflection and transmission spectra, after smoothing (polynomial order: 3 and smoothing points: 7), baseline correction and mean centering: Score values of the first principal component for sample #1 (a) and #2 (b) and loading spectra of the first principal component (c). In SM5 are available full PCAs with two components.

In order to continue with the study of the differences between the transflection and transmission measurements but avoiding the effect of the tissue thickness, a new PCA (See Figure 5) was performed after normalizing and baseline correction. In the case of sample #1 the first scores plot showed strong differences between the transflection and transmission spectra, but in sample #2 those differences were shown especially on the score 2, which captures 33% of the variance. Again, score values of the transflection spectra also show more variance as compared to the transmission ones. Loading plots corresponding to those scores (see Figure 5c) revealed that the main differences between transflection and

transmission spectra are connected with a shift of the amide I band, as evidenced by the derivative shape in the region between 1700-1600 cm^{-1}. Since the score values of the transflection are higher than those of the transmission, it can be concluded that the band in the transflection mode is shifted to higher wavenumber values. For the transflection spectra, the mean (± standard deviation) maximum of the band was located at 1657.9 ± 1.4 and 1656 ± 3 cm^{-1} for tissues #1 and #2 respectively, while for transmission measurements the mean maximum was located at 1654 ± 1 cm^{-1} and 1655.5 ± 1.4 cm^{-1} for tissues #1 and #2, respectively. Other significant loadings are observed for the symmetric and asymmetric phosphodiester vibrations at ~1240 cm^{-1} and ~1085 cm^{-1} in the case of transflection measurements.

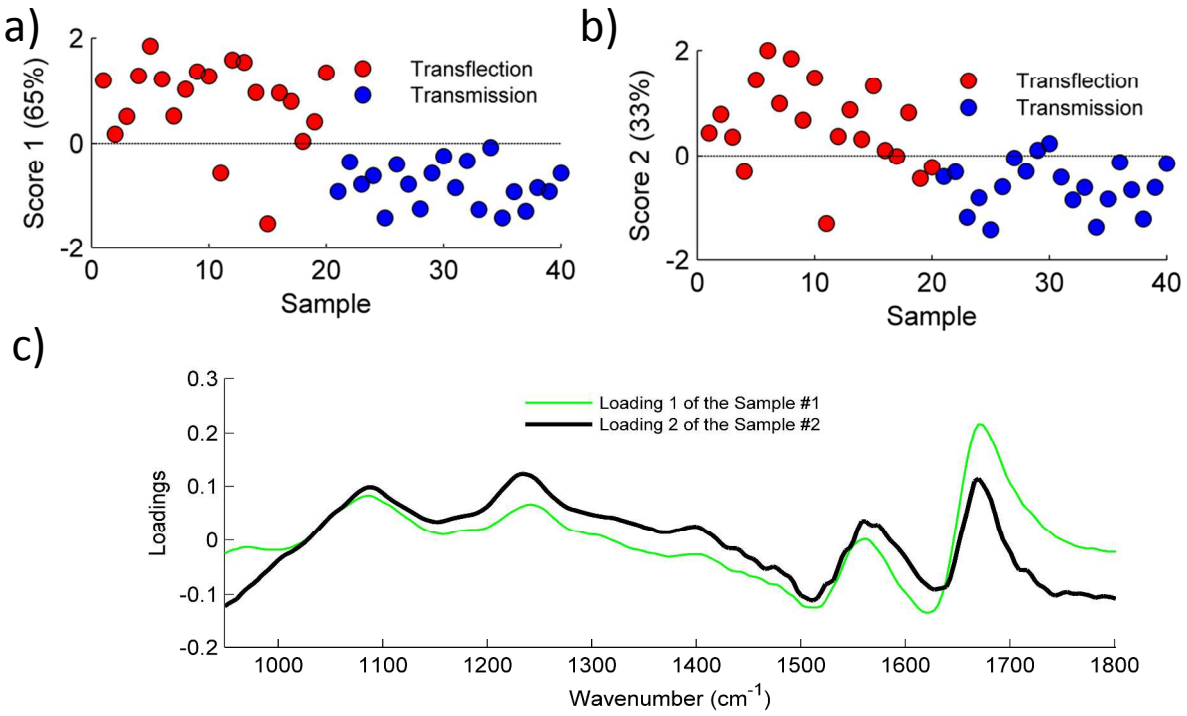

Figure 5. PCA performed over the transflection and transmission spectra, after smoothing (polynomial order: 0 and smoothing points: 7), baseline correction, normalization (Whole area = 1) and mean centering: Score values for the first principal component for sample #1 (a) and second principal component for sample #2 (b) and loading spectra of the principal components (c). NOTE: Loading spectra were shifted on the y-axis. Complete PCAs with two components are shown in Supplementary Figure 5.

The 2 or 3 wavenumber value shift observed for the transflection measurements was small as compared with the spectral resolution (4cm^{-1}) used for the measurements. This shift on the amide I in transflection spectrum has been also observed by Bassan et al.[9] in cytosine films and by Wehbe

.[13] in cell cultures, being assigned in both studies this shift to EFWS. Other sources could contribute to spectral shifts of these magnitudes such as differences in scattering[14] such as dispersion due to the different thicknesses of the transflection and transmission tissues. According to Bassan et al., the Mie scattering is identified "as a sharp decrease in intensity on the high wavenumber side of absorption bands, in particular the Amide I band at 1655 cm^{-1}, causing a downward shift of the true peak position".[15] This description fits nicely with our observations, specially taking into account that the Mie scattering is particle size-dependent and that the tissues employed for transmission were cut with a thickness two times higher than the tissue employed for the transflection spectra.

Another explanation could be found in the reflection contribution to the transflection spectra recently observed by Bassan et al.[16] that demonstrated that all the spectra obtained in transflection mode is a weighted sum of the reflection and transmission modes. In the case of this study, the amide I band of the transflection spectra were blue-shifted compared to the transmission mode, which could be explained by a contribution from the reflection component that was absent in the transmission measurements.

Conclusions

Our results demonstrated that in the case of the lymphoma tissue under study, the presence of the transflection "artifacts" were not critical and that transflection spectra were comparable to transmission spectra after a standard preprocessing. An overall inspection of the hyperspectral images using cluster analysis showed that the regions of the tissue were grouped according to tissue fixation effects instead of the measurement mode –transflection or transmission- employed for the image acquisition. A more detailed examination of the peripheral tissue zone indicated some differences between the transflection and transmission spectra such as a small shift of the amide I of 2-3 wavenumber values and a large variance in the case of the transflection spectra. Both effects can be related to EFWS and, although they are consistent across the peripheral tissue zone, the noise introduced noise makes mandatory averaging of several spectra of the same region of the tissue if a representative spectrum of the region was required.

Although these results cannot be directly extended to other tissues or other spectral regions, they support the use of cost-effective transflection measurements for diagnostic purposes and/or

structural studies, despite the fact that always a proper evaluation of the impact of those artefacts on the target tissue should be performed prior to any general study. For this propose we recommend the straightforward and simple methodology used in this study, based on the multivariate comparison of images and spectra from transmission and transflection measurements obtained from adjacent sections of tissues before the routine use of the transflection substrates.

Acknowledgements

Authors gratefully acknowledge the financial support of the Ministerio de Economía y Competitividad and FEDER (Projects **CTQ2011-25743** and **2012-38635**) and the Generalitat Valenciana (Project PROMETEO **2010-055**). DPG acknowledges the "V Segles" grant provided by the University of Valencia enabling a research stay at the Monash University. A/Prof. B. R. Wood is funded by an Australia Research Council Discovery Future Fellowship (FT120100926) and the research is supported by an ARC Discovery grant (DP120100431). We thank Mr. Finlay Shanks (Monash University) for the instrumental support.

References.

1. C. Kendall, M. Isabelle, F. Bazant-Hegemark, J. Hutchings, L. Orr, J. Babrah, R. Baker, and N. Stone, *Analyst*, 2009, **134**, 1029–1045.
2. S. L. Haas, R. Muller, A. Fernandes, K. Dzeyk-Boycheva, S. Wurl, J. Hohmann, S. Hemberger, E. Elmas, M. Bruckmann, P. Bugert, and J. Backhaus, *Appl. Spectrosc.*, 2010, **64**, 262–267.
3. K. T. Cheung, J. Trevisan, J. G. Kelly, K. M. Ashton, H. F. Stringfellow, S. E. Taylor, M. N. Singh, P. L. Martin-Hirsch, and F. L. Martin, *Analyst*, 2011, **136**, 2047–2055.
4. K. Malek, B. R. Wood, and K. R. Bambery, in Optical Spectroscopy and Computational Methods in Biology and Medicine, ed. M. Baranska, Springer Netherlands, 2014, pp. 419–473.
5. J. Filik, M. D. Frogley, J. K. Pijanka, K. Wehbe, and G. Cinque, *Analyst*, 2012, **137**, 853–861.
6. H. Brooke, B. V. Bronk, J. N. utcheon, S. L. Morgan and M. L. Myrick, *Appl. Spectrosc.* , 2009, **63**, 1293–1302.
7. O. Wiener, *Ann.Phys.*, 1890, **40**, 203.
8. R.G.Greenler *J. Chem. Phys.,* 1966, **44**, 310-315

9. P. Bassan, J. Lee, A. Sachdeva, J. Pissardini, K. M. Dorling, J. S. Fletcher, A. Henderson, and P. Gardner, *Analyst*, 2013, **138**, 144–157.
10. T. P. Wrobel, B. Wajnchold, H. J. Byrne, and M. Baranska, *Vib. Spectrosc*., 2013, **69**, 84–92.
11. B. R. Wood, K. R. Bambery, C. J. Evans, M. A. Quinn, and D. McNaughton, *BMC Med. Imaging*, **6**, 12.
12. P. Lasch, Cytospec, 2000.
13. K. Wehbe, J. Filik, M. D. Frogley, G. Cinque, *Anal. Bioanal. Chem.*, 2013, **405**, 1311,1324.
14. H. Brooke, D. L. Perkins, B. Setlow, P. Setlow, B. V. Bronk and M. L. Myrick, Appl. Spectrosc. , 2008, **62**, 881–888.
15. P. Bassan, A. Kohler, H. Martens, J. Lee, H. J. Byrne, P. Dumas, E. Gazi, M. Brown, N. Clarke, and P. Gardner, *Analyst*, 2010, **135**, 268–277.
16. P. Bassan, H. J. Byrne, J. Lee, F. Bonnier, C. Clarke, P. Dumas, E. Gazi, M. D. Brown, N. W. Clarke, and P. Gardner, *Analyst*, 2009, **134**, 1171–1175.

Table of contents: FTIR microscopy of adjacent sections of tissue measured by transmission and transflection shows comparable images after UHCA.